SUMMARY OF THE FINDINGS OF MINOR RESEARCH PROJECT (MRP)

Title of MRP: Synthesis and characterization of Ni and Mn doped $MgFe_2O_4$ metal oxide used for supercapacitor application

UGC approval No. and Date: F.47-763/13 (WRO) Dated – 20th March 2014

Principal Investigator: Mr. Santosh J. Uke, Department of Physics,
J. D. Patil Sangludkar Mahavidhyalay, Daryapur, Dist Amravati, Pin 444705,
Maharashtra.

SUMMARY OF THE FINDINGS

Energy plays a major role in improving the human living standard, which ultimately helps in the development of any nation. For implementation of advanced technology in different sectors like industry, agriculture, medical, social, etc. in rural as well as urban areas, the major requirement is the energy. Energy storage is as equal as energy production. Furthermore, the energy storage of low unit to very high unit is a very difficult task for an existed energy storage technology.

The supercapacitor is an energy storage device. It is bridging the gap between conventional capacitor energy storage technology and battery energy storage technology. Supercapacitor is very attractive amongst other energy storage devices because of its light weight, environmentally friendly, inexpensive energy storage, maintenance free, long life operation, high energy density and high power density. Supercapacitor has wider applications, it is used in hybrid vehicles, power backup, military services and portable electronics such as laptops, mobile phones, wrist watches, wearable devised, roll-up displays electronic papers, etc

Considering the above mention discussion, we planned to study and synthesized energy storage material for the electrode in supercapacitor. In the first year of the

project work, we reviewed the literature on supercapacitor. Based on this literature review, we published a research paper in Frontiers in material Journal. For an experimental work, initially, we synthesized Ni and Mn doped $MgFe_2O_4$ and studies its supercapacitive properties. Furthermore, we doped Zn in $MgFe_2O_4$. From this combination, we got nanosize, spherical morphology of the Zn in $MgFe_2O_4$. The Zn doped $MgFe_2O_4$ resulted into a large specific capacitance, high energy density and cyclic stability. For 2 atomic wt % Zn doped $MgFe_2O_4$, the specific capacitance of 406.25 Fg^{-1} and energy density 8.75 $WhKg^{-1}$ can be achieved at the current density of 1$mAcm^{-2}$. For the publication of this result, we had submitted our manuscript in the 'Electrochemical Acta' an Elsevier Journal, but these journals suggested little improvement in the study and reject this paper. After improvement, further we have submitted this manuscript into Journal 'Engineering Science and Technology, An International Journal' for publication.

As this project work is also enrolled for Ph.D. at Sant Gadge Baba Amravati University, Amravati, Maharashtra. For the Ph.D. work, we have synthesized and characterized $NiCo_2O_4$ and $MnCo_2O_4$ via sol-gel method and studied its electrochemical properties for supercapacitor applications. From this study, we got high surface area with large porous electrode material. In the consequences the $NiCo_2O_4$ and $MnCo_2O_4$ materials resulted into a specific capacitance of 342 Fg^{-1} and 42.5 Fg^{-1} respectively. The obtain results we have published in an international Journals. The list of publications from this project work is as follows.

1. "Recent Advancements in the Cobalt Oxides, Manganese Oxides, and Their Composite As an electrode Material for Supercapacitor: A Review." **Uke, S.**

J., Akhare, V. P., Bambole, D. R., Bodade, A. B., & Chaudhari, G. N. (2017). *Frontiers*, *4*(21), 1.

2. "Fabrication of Spherical Nanocrystalline $MnCo_2O_4$ Via Sol- Gel Citrate Route For Supercapacitor Application" **Uke S. J**., Akhare V. P., Meshram S. P., Bambole, D. R., Thakre D. S., & Chaudhari, G. N. (2018).. *International Journal of Science and Research (IJSR),* 5(1), 254-561
3. "Cost effective synthesis of spinel $NiCo_2O_4$ nanocrystal by sol-gel citrate method and its application for supercapacitor". **Uke, S. J**., Akhare, V. P., Bambole, D. R., Bodade, A. B., Chaudhari, G. N., *International Journal of Materials Science* ISSN 0973-4589 Volume 12, Number 2 (2017), pp. 371-377

Mr. Santosh J. Uke

frontiers in Materials

MINI REVIEW
published: 02 August 2017
doi: 10.3389/fmats.2017.00021

Recent Advancements in the Cobalt Oxides, Manganese Oxides, and Their Composite As an Electrode Material for Supercapacitor: A Review

Santosh J. Uke[1,2], Vijay P. Akhare[2], Devidas R. Bambole[1], Anjali B. Bodade[2] and Gajanan N. Chaudhari[2]*

[1]*J. D. Patil Sangludkar College, Daryapur, India,* [2]*Nanoscience Research Laboratory, Shri Shivaji Science College, Amravati, India*

Recently, our modern society demands the portable electronic devices such as mobile phones, laptops, smart watches, etc. Such devices demand light weight, flexible, and low-cost energy storage systems. Among different energy storage systems, supercapacitor has been considered as one of the most potential energy storage systems. This has several significant merits such as high power density, light weight, eco-friendly, etc. The electrode material is the important part of the supercapacitor. Recent studies have shown that there are many new advancement in electrode materials for supercapacitors. In this review, we focused on the recent advancements in the cobalt oxides, manganese oxides, and their composites as an electrode material for supercapacitor.

Keywords: hybrid supercapacitor, cobalt oxide, manganese oxide, specific capacitance, specific surface area

OPEN ACCESS

Edited by:
Sravendra Rana, University of Petroleum and Energy Studies, India

Reviewed by:
Zhengjun Zhang, Tsinghua University, China
Hongchang Pang, Dalian University of Technology (DUT), China

****Correspondence:***
Santosh J. Uke
santosh_uke@rediffmail.com

Specialty section:
This article was submitted to Nanoenergy Technologies and Materials, a section of the journal Frontiers in Materials

Received: *10 February 2017*
Accepted: *30 June 2017*
Published: *02 August 2017*

Citation:
Uke SJ, Akhare VP, Bambole DR, Bodade AB and Chaudhari GN (2017) Recent Advancements in the Cobalt Oxides, Manganese Oxides, and Their Composite As an Electrode Material for Supercapacitor: A Review. Front. Mater. 4:21. doi: 10.3389/fmats.2017.00021

INTRODUCTION

Energy storage has an equal importance as energy production. To face the global challenges, recently, our modern society demands lightweight, flexible, inexpensive, and environmentally friendly energy storage systems (Meng et al., 2010; Chodankar et al., 2015). Battery and supercapacitor are the major energy storage devices. But, slow charge–discharge rate, short life cycles, and high weight of battery limit its applications in portable and wearable devises (Meng et al., 2010). At present, supercapacitors have been receiving a great attention, because of their important features such as high energy density, high power density, light weight, fast charging–discharging rate, secure operation, and long life span (Jayalakshmi and Balasubramanian, 2008; Chodankar et al., 2015). The supercapacitor is also called electrochemical capacitor. This is used in various applications such as hybrid vehicles, power backup, military services, and portable electronic devises like laptops, mobile phones, wrist watches, wearable devised, roll-up displays electronic papers, etc. (Lee et al., 2011; Wang et al., 2012).

CLASSIFICATION OF THE SUPERCAPACITOR

On the basis of charge storage mechanism and material used as the electrode, the supercapacitors are divided into two categories: electrochemical double layer supercapacitors (EDLCs) and pseudocapacitor (Jayalakshmi and Balasubramanian, 2008). In EDLCs, the specific capacitance arises from the non-Faradaic charge storage mechanism between electrode and electrolyte interface (Jayalakshmi and Balasubramanian, 2008; Wang et al., 2012). The materials that have been used as electrode

for EDLCs are porous carbon (Kang et al., 2015), SWNT (Liu et al., 2006), MWNT (Huang et al., 2014a), reduce graphine oxide (Zhang and Zhao, 2012), aerogel (Faraji and Ani, 2015), etc. In pseudocapacitor, the specific capacitance arises from Faradaic reaction at the electrode interface. The materials that have been studied as electrode for pseudocapacitors are transition metal oxides and conducting polymers (Wang et al., 2012).

In particular, the specific capacitance of the supercapacitors depends on the surface area and the pore size distribution of the electrode material. Compared with the transition metal oxides and conducting polymers, carbon and its different types have high surface area (3.270 m^2g^{-1}) (Kang et al., 2015). However, this high surface area of carbon is not completely accessible for the electrolyte (Faraji and Ani, 2015). To overcome this shortcoming, the composites of carbon with transition metal oxides or conducting polymer have received great attention. These composite are also called hybrid materials. The use of hybrid material as an electrode in supercapacitors result in the third category of supercapacitors called hybrid supercapacitors. In hybrid supercapacitors, the specific capacitance arises from Faradic as well as non-Faradic charge storage mechanism at the electrode and electrolyte interface (Zhang et al., 2013; Pardieu et al., 2015).

PARAMETERS FOR SUPERCAPACITOR

The specific capacitance (C_s) (Fg^{-1}), energy density E (Wh kg^{-1}), power density P (kW kg^{-1}), and retention capacity or coulomb efficiency (η) are the crucial characteristics of the supercapacitor device. The (C_s) (Fg^{-1}) at the single electrode of the device is calculated given by,

$$C_s = \frac{1}{mV(V_c - V_a)} \int_{v_a}^{v_c} I(v)dV \quad (1)$$

where m is the mass (g cm^{-1}) deposited, $I(v)$ is the response current (mA) of the electrode material for unit area, V is the scan rate, $V_c - V_a$ is the operational potential window in (V), V_a anodic current, and V_c cathodic current. Energy density E (Wh kg^{-1}) and power density P (W kg^{-1}) of supercapacitor are calculated using following relations as,

$$E = \frac{0.5 \times C_s \times (V_{max}^2 - V_{min}^2)}{3.6} \quad (2)$$

$$P = \frac{E}{t_D} \quad (3)$$

where C_s is specific capacitance (Fg^{-1}), V_{max} and V_{min} are the maximum and minimum voltage achieved during charging and discharging process, respectively, in volt (V), and t_D is the discharging time (s) for a cycle of the supercapacitor. The retention of specific capacitance is calculated using the relation,

$$\eta = \frac{t_D}{t_C} \quad (4)$$

where t_C and t_D are the charge and discharge time (s), respectively, for a cycle of the supercapacitor (Wang et al., 2010; Dubal et al., 2012).

RECENT ADVANCES IN COBALT OXIDE SUPERCAPACITOR

The transition metal oxides have a great scientific significance. These are the basis of a variety of functional materials (Shinde et al., 2015). Among the various supercapacitor electrode materials, transition metal oxides offer high electronegativity, rich redox reactions, low cost, environmental friendliness, and excellent electrochemical performance. Different transition-metal oxides, such as IrO_2, RuO_2, Co_3O_4, MnO_2, Fe_2O_3, SnO_2,

TABLE 1 | Co_3O_4-based supercapacitors.

Sr. no.	Material	Method of synthesis	High surface area	Electrolyte	High Sp. capacitance	Retention	Year	Reference
1	Co_2O_3 on NiO substrate	Electrodeposition method		1 M KOH	345 Fg^{-1} at 20 mV s^{-1}	>50% after 200	2014	Sarma et al. (2014)
2	Co_3O_4-decorated graphene	Microwave-assisted method	–	1 M KOH	600 Fg^{-1} at 0.7 A g^{-1}	94.5% after 5,000 cycles	2015	Kumar et al. (2015)
3	Pongam seed shell-derived activated carbon and cobalt oxide (Co_3O_4) nanocomposite	KOH activation method	164 m^2 g^{-1}	1 M KOH electrolyte	94 Fg^{-1} at 1 A g^{-1}	88% after 1,000 cycles	2015	Madhu et al. (2015)
4	Co_3O_4/$NiCo_3O_4$ double-shelled nanocages	The facile synthesis	–	2 M KOH	972 Fg^{-1} at a current density of 5 A g^{-1}	92.5% after 12,000 cycles	2015	Hu et al. (2015)
5	Synthesized titania nanotube cobalt (CoS) sulfide composite	Electrodeposition method	–	1 M Na_2SO_3	400 Fg^{-1} at charge density 5 mA cm^{-2}	>80% after 1,000 cycles	2015	Ray et al. (2015)
6	Co_3O_4 nanotubes	Chemical deposition method		6 ML^{-1} KOH	574 Fg^{-1} at 0.1 A g^{-1}	95% after 1,000 cycles	2010	Xu et al. (2010)
7	Ultrafine Co_3O_4 nanocrystal electrode	Laser ablation in liquid method	–		177 Fg^{-1} at scan rate 1 mV s^{-1}	100% after 20,000 cycles	2016	Liu et al. (2016)
8	Cobalt tungstate ($CoWO_4$)	Chemical precipitation reaction	–	0.2 M H_2SO_4	378 Fg^{-1} at scan rate 2 mV s^{-1}	95.5% after 4,000 cycles	2016	Adib et al. (2016)

NiO, etc., have been extensively studied as the electrode material for supercapacitor (Luo et al., 2014). Among these, RuO_2 has been identified as a dominant candidate because it has high theoretical specific capacitance (1,358 Fg^{-1}), high electrical conductivity (300 S cm^{-1}), and high electrochemical stability (Yu et al., 2013). However, the high cost and toxicity associated with the RuO_2 limits its commercial applications (Deng et al., 2014).

Furthermore, the cobalt oxides have received significant interest in recent years because of their low cost, non-toxic, easy synthesis, and environmental friendly nature. The cobalt oxides have high theoretical capacitance (CoO: 4.292 Fg^{-1}, Co_2O_4: 3.560 Fg^{-1}) (Cheng et al., 2010; He et al., 2012). Additionally, cobalt oxides show excellent electrochemical behavior in alkaline as well as organic electrolyte. These have the ability to interact with the ions of the electrolyte at the surface as well as through the bulk of the material (Vijayakumar et al., 2013). The features of cobalt oxides such as morphology, structures, and dimension can be easily controlled *via* adjusting the preparative parameters such as, reaction temperature, reaction time, concentration of matrix solution, complexing agent, etc. (Wei et al., 2015a).

An optimize microstructure and controlled morphology of the material will enhance the specific surface area and pore size distribution, which facilitate the electrolyte ion transport in the material (Meher and Rao, 2011). Recently, many new approaches have been successfully in use to synthesize the meso and microporous nanostructure cobalt oxide materials such as hydrothermal method (Meher and Rao, 2011), chemical bath deposition method (Xu et al., 2010), hydrothermal precipitation method (Yu et al., 2009), solvothermal synthesis method (Yang et al., 2013), combustion synthesis method (Deng et al., 2014), microwave-assisted synthesis method (Vijayakumar et al., 2013), etc.

The specific capacitance of the cobalt oxide strongly depends on morphology, surface area, and pore size distribution. Recently,

TABLE 2 | MnO_2-based supercapacitor.

Sr. no.	Material	Method of synthesis	High surface area	Electrolyte	High Sp. capacitance	Retention	Year	Reference
1	Manganese oxide (MnO_2)/three-dimensional (3D) reduced graphene oxide (RGO)	Reverse microemulsion (water/oil) method	142 $m^2 g^{-1}$	0.1 M Na_2SO_4	709.8 Fg^{-1} at 0.2 A g^{-1}	97.6% after 1,000 cycles	2015	Wei et al. (2015b)
2	Coaxial mesoporous MnO_2/amorphous-carbon nanotubes	Redox reaction between $KMnO_4$ and amorphous carbon nanotube in acid solution	–	1 M Na_2SO_4	362 Fg^{-1} at the current density of 0.5 A g^{-1}	88.6% after 3,000 cycles	2015	Zhu et al. (2015)
3	3D porous CNT/MnO_2 composite	Dipping and drying process followed by a potentionstatic deposition technology	230.85 $m^2 g^{-1}$	0.5 M NaOH	160.5 Fg^{-1} at the current density of 1 A^{-1}	–	2015	Guo et al. (2015b)
4	Carbon nanosheets supported MnO_2	Carbonization and reduction method	573 $m^2 g^{-1}$	6 M KOH	656 Fg^{-1} at a current density of 1 A g^{-1}	80% after 5,000 cycles	2015	Sun et al. (2015)
5	A RGO/manganese dioxide (MnO_2)/silver nanowire ternary hybrid film	A facile vacuum filtration and subsequent thermal reduction	–	0.5 M Na_2SO_4	4.42 F cm^{-3} at a scan rate of 10 mV s^{-1}	90.3% after 6,000 cycles	2015	Liu et al. (2015)
6	Three-dimensional carbon nanotubes@ MnO_2 core shell nanostructures	A floating catalyst chemical vapor deposition process and a facile hydrothermal approach	127.5 $m^2 g^{-1}$	1 M Na_2SO_4	325.5 F g^{-1} at a current density of 0.3 A g^{-1}	90.5% after 5,000 cycles	2014	Huang et al. (2014b)
7	MnO_2/Graphine argogel composites	Graphene aerogels: an organic sol-gel process and MnO_2 electrochemically deposit on GA	793 $m^2 g^{-1}$	0.5 M Na_2SO_4	410 Fg^{-1} at 2 mV s^{-1}	95% after 50,000 cycles at 1,000 mV s^{-1}	2014	Wang et al. (2014)
8	Manganese oxide nanosheets/ nanoporous gold	Galvanostatic electrodepositon	–	1 M Na_2SO_4	775 Fg^{-1} at 1 A g^{-1}	95% after 1,000 cycles	2015	Zeng et al. (2015)
9	MnO_2 on graphene	Hydrothermal method	–	1 M Na_2SO_4	315 Fg^{-1} at a current density of 0.2 A g^{-1}	87% retained after 2,000 cycles at 3 A g^{-1}	2013	Liu et al. (2013)
10	MnO_2 nanosheets on flexible carbon fiber cloth	Flexible carbon fiber cloth: the direct carbonization of flax textile redox reaction between carbon and $KMnO_4$	33.6 $m^2 g^{-1}$	0.1 M Na_2SO_4	683.73 Fg^{-1} at 2 A g^{-1}	94.5% retained after 2,000 cycles	2015	He and Chen (2015)

use of new synthesis approaches, surface modifying agents, complexing, and structure directing agent results in high-specific capacitance, which is equal the theoretical specific capacitance cobalt oxide. In this review paper, we have focused the recent advancements in the cobalt oxides and their composites as the electrode material. **Table 1** shows the preparation and supercapacitive performance of cobalt oxide and their composites based supercapacitors.

RECENT ADVANCES IN MANGANESE OXIDE SUPERCAPACITOR

Manganese (Mn) has different oxidation states. Out of these, the most stable oxidation states are Mn (II) and Mn (IV). The Mn (II) forms MnO, on the other hand, Mn (IV) forms MnO_2 and Mn_2O_3. The MnO_2 has α, β, γ, and δ -type polymorph (Chen et al., 2014; Salunkhe et al., 2015). The advantages of manganese-based metal oxides include low cost, low toxicity, natural abundance, and environmental friendly in nature (Sui et al., 2015; Wei et al., 2015b). In aqueous and organic electrolyte, the MnO, MnO_2, and Mn_2O_3 can form the different oxidation states. Thus, it results in the high-specific capacitance. The highest reported theoretical specific capacitance of MnO_2 is 1.370 Fg^{-1} (Guo et al., 2015a; Wei et al., 2015b). However, the low electrical conductivity and large volume change during the charge–discharge process result in the unsatisfactory rate performance and cyclic stability. In consequence, this reduces the specific capacitance of the manganese oxides-based supercapacitors (Cabana et al., 2010; Chen et al., 2010). To overcome such hindrances, recently, the researchers have been executing many new strategies, such as use of carbon containing materials for increasing the electrical conductivity and adopt the volume buffers for relaxing internal stresses (Yao et al., 2008; Sui et al., 2015). Manganese oxides have been prepared by various synthesis methods, such as pulse laser deposition method (Xia et al., 2011), hydrothermal method (Zhang et al., 2014), electrochemical synthesis method (Jiang and Kucernak, 2002), redox deposition method (Bordjiba and Bélanger, 2009), successive hydrolysis–condensation method (Sawangphruk and Limtrakul, 2012), etc. Further, the detail of MnO_2 synthesis and their supercapacitive performance are shown in **Table 2**.

CONCLUSION AND FUTURE PROSPECTIVE

Recently, cobalt- and manganese-based metal oxide as the electrode materials for supercapacitor have been receiving the great attention. From the recent reports, it has concluded that,

(1) Advanced chemical method such as hydrothermal, pulse laser deposition, reverse microemulsion, microwave-assisted, etc., has been assisted to synthesize cobalt- and manganese-based metal oxide material.
(2) The specific capacitance of the cobalt oxide- and manganese-based metal oxide supercapacitor strongly depends on morphology, surface area, and pore-size distribution.
(3) In most of the reports, the composites of cobalt oxide or manganese oxide with carbon material, i.e., hybrid materials are used as an electrode for supercapacitor. Moreover, this results in high-specific capacitance.
(4) In addition, the increase in conductivity of the cobalt oxide and manganese oxides is projected if this material and carbon material are combined. This makes the application of cobalt oxide and manganese oxides in high energy applications. As a result, the proposed material cobalt oxides and manganese oxide are a promising material for flexible, portable high-rate hybrid supercapacitor, and has plenty room for advancements.

AUTHOR CONTRIBUTIONS

All authors listed have made a substantial, direct, and intellectual contribution to the work and approved it for publication.

FUNDING

This work is financially supported by University Grant Commission (UGC) New Delhi, India under Minor Research Project (File No.47-763/13/WRO).

REFERENCES

Adib, K., Rahimi-Nasrabadi, M., Rezvani, Z., Pourmortazavi, S. M., Ahmadi, F., Naderi, H. R., et al. (2016). Facile chemical synthesis of cobalt tungstates nanoparticles as high performance supercapacitor. *J. Mater. Sci. Mater. Electron.* 27, 4541. doi:10.1007/s10854-016-4329-4

Bordjiba, T., and Bélanger, D. (2009). Direct redox deposition of manganese oxide on multiscaled carbon nanotube/microfiber carbon electrode for electrochemical capacitor. *J. Electrochem. Soc.* 156, A378–A384. doi:10.1149/1.3090012

Cabana, J., Monconduit, L., Larcher, D., and Palacin, M. R. (2010). Beyond intercalation-based Li-Ion batteries: the state of the art and challenges of electrode materials reacting through conversion reactions. *Adv. Mater. Weinheim* 22, 35. doi:10.1002/adma.201000717

Chen, I. L., Chen, T. Y., Wei, Y. C., Hu, C. C., and Lin, T. L. (2014). Capacitive performance enhancements of RuO_2 nanocrystals through manipulation of preferential orientation growth originated from the synergy of Pluronic F127 trapping and annealing. *Nanoscale* 6, 2861–2871. doi:10.1039/c3nr04479c

Chen, S., Zhu, J., Wu, X., Han, Q., and Wang, X. (2010). Graphene oxide-MnO_2 nanocomposites for supercapacitors. *ACS Nano* 4, 2822–2830. doi:10.1021/nn901311t

Cheng, H., Lu, Z. G., Deng, J. Q., Chung, C. Y., Zhang, K., and Li, Y. Y. (2010). A facile method to improve the high rate capability of Co_3O_4 nanowire array electrodes. *Nano Res.* 3, 895–901. doi:10.1007/s12274-010-0063-z

Chodankar, N. R., Dubal, D. P., and Gund, G. S. (2015). Flexible all-solid-state MnO_2 thin films based symmetric supercapacitors. *Electrochim. Acta* 165, 338–347. doi:10.1016/j.electacta.2015.02.246

Deng, J., Kang, L., Bai, G., Li, Y., Li, P., Liu, X., et al. (2014). Solution combustion synthesis of cobalt oxides (Co_3O_4 and Co_3O_4/CoO) nanoparticles as supercapacitor electrode materials. *Electrochim. Acta* 132, 127–135. doi:10.1016/j.electacta.2014.03.158

Dubal, D. P., Kim, W. B., and Lokhande, C. D. (2012). Galvanostatically deposited Fe: MnO_2 electrodes for supercapacitor application. *J. Phys. Chem. Solids* 73, 18–24. doi:10.1016/j.jpcs.2011.09.005

Faraji, S., and Ani, F. N. (2015). The development supercapacitor from activated carbon by electroless plating – a review. *Renew. Sustain. Energ. Rev.* 42, 823–834. doi:10.1016/j.rser.2014.10.068

Guo, W. H., Liu, T. J., Jiang, P., and Zhang, Z. J. (2015a). Free-standing porous manganese dioxide/graphene composite films for high performance supercapacitors. *J. Colloid Interface Sci.* 437, 304–310. doi:10.1016/j.jcis.2014.08.060

Guo, C., Li, H., Zhang, X., Huo, H., and Xu, C. (2015b). 3D porous CNT/MnO_2 composite electrode for high-performance enzymeless glucose detection and supercapacitor application. *Sens. Actuators B Chem.* 206, 407–414. doi:10.1016/j.snb.2014.09.058

He, G., Li, J., Chen, H., Shi, J., Sun, X., Chen, S., et al. (2012). Hydrothermal preparation of Co_3O_4@ graphene nanocomposite for supercapacitor with enhanced capacitive performance. *Mater. Lett.* 82, 61. doi:10.1016/j.matlet.2012.05.048

He, S., and Chen, W. (2015). Application of biomass-derived flexible carbon cloth coated with MnO_2 nanosheets in supercapacitors. *J. Power Sources* 294, 150–158. doi:10.1016/j.jpowsour.2015.06.051

Hu, H., Guan, B., Xia, B., and Lou, X. W. (2015). Designed formation of Co_3O_4/$NiCo_2O_4$ double-shelled nanocages with enhanced pseudocapacitive and electrocatalytic properties. *J. Am. Chem. Soc.* 137, 5590–5595. doi:10.1021/jacs.5b02465

Huang, K. J., Wang, L., Zhang, J. Z., Wang, L. L., and Mo, Y. P. (2014a). One-step preparation of layered molybdenum disulfide/multi-walled carbon nanotube composites for enhanced performance supercapacitor. *Energy* 67, 234–240. doi:10.1016/j.energy.2013.12.051

Huang, M., Zhang, Y., Li, F., Zhang, L., Wen, Z., and Liu, Q. (2014b). Facile synthesis of hierarchical Co_3O_4@MnO_2 core-shell arrays on Ni foam for asymmetric supercapacitors. *J. Power Sources* 252, 98–106. doi:10.1016/j.jpowsour.2013.12.030

Jayalakshmi, M., and Balasubramanian, K. (2008). Simple capacitor to supercapacitor – an overview. *Int. J. Electrochem. Sci.* 11, 1196–1217.

Jiang, J., and Kucernak, A. (2002). Electrochemical supercapacitor material based on manganese oxide: preparation and characterization. *Electrochim. Acta* 47, 2381–2386. doi:10.1016/S0013-4686(02)00031-2

Kang, D., Liu, Q., Gu, J., Su, Y., Zhang, W., and Zhang, D. (2015). "Egg-box"-assisted fabrication of porous carbon with small mesopores for high-rate electric double layer capacitors. *ACS Nano* 9, 11225–11233. doi:10.1021/acsnano.5b04821

Kumar, R., Singh, R. K., Dubey, P. K., Singh, D. P., and Yadav, R. M. (2015). Self-assembled hierarchical formation of conjugated 3D cobalt oxide nanobead–CNT–graphene nanostructure using microwaves for high-performance supercapacitor electrode. *ACS Appl. Mater. Interfaces* 7, 15042–15051. doi:10.1021/acsami.5b04336

Lee, S. W., Gallant, B. M., Byon, H. R., Hammond, P. T., and Shao-Horn, Y. (2011). Nanostructured carbon-based electrodes: bridging the gap between thin-film lithium-ion batteries and electrochemical capacitors. *Energy Environ. Sci.* 4, 1972–1985. doi:10.1039/c0ee00642d

Liu, W., Lu, C., Wang, X., Tay, R. Y., and Tay, B. K. (2015). High-performance microsupercapacitors based on two-dimensional graphene/manganese dioxide/silver nanowire ternary hybrid film. *ACS Nano* 9, 1528–1542. doi:10.1021/nn5060442

Liu, X. Y., Gao, Y. Q., and Yang, G. W. (2016). A flexible, transparent and super-long-life supercapacitor based on ultrafine Co_3O_4 nanocrystal electrodes. *Nanoscale* 8, 4227–4235. doi:10.1039/C5NR09145D

Liu, Y., Yan, D., Zhuo, R., Li, S., Wu, Z., Wang, J., et al. (2013). Design, hydrothermal synthesis and electrochemical properties of porous birnessite-type manganese dioxide nanosheets on graphene as a hybrid material for supercapacitors. *J. Power Sources* 242, 78–85. doi:10.1016/j.jpowsour.2013.05.062

Liu, T., Kumar, S., Inventors; Georgia Tech Research Corporation, Assignee. (2006). *Supercapacitor Having Electrode Material Comprising Single-Wall Carbon Nanotubes and Process for Making the Same*. United States patent US 7,061,749.

Luo, Y., Zhang, H., Guo, D., Ma, J., Li, Q., Chen, L., et al. (2014). Porous $NiCo_2O_4$-reduced graphene oxide (rGO) composite with superior capacitance retention for supercapacitors. *Electrochim. Acta* 132, 332–337. doi:10.1016/j.electacta.2014.03.179

Madhu, R., Veeramani, V., Chen, S. M., Manikandan, A., Lo, A. Y., and Chueh, Y. L. (2015). Honeycomb-like porous carbon-cobalt oxide nanocomposite for high-performance enzymeless glucose sensor and supercapacitor applications. *ACS Appl. Mater. Interfaces* 7, 15812–15820. doi:10.1021/acsami.5b04132

Meher, S. K., and Rao, G. R. (2011). Effect of microwave on the nanowire morphology, optical, magnetic, and pseudocapacitance behavior of Co_3O_4. *J. Phys. Chem. C* 115, 25543–25556. doi:10.1021/jp209165v

Meng, C., Liu, C., Chen, L., Hu, C., and Fan, S. (2010). Highly flexible and all-solid-state paperlike polymer supercapacitors. *Nano Lett.* 10, 4025–4031. doi:10.1021/nl1019672

Pardieu, E., Pronkin, S., Dolci, M., Dintzer, T., Pichon, B. P., Begin, D., et al. (2015). Hybrid layer-by-layer composites based on a conducting polyelectrolyte and Fe_3O_4 nanostructures grafted onto graphene for supercapacitor application. *J. Mater. Chem. A* 3, 22877–22885. doi:10.1039/C5TA05132K

Ray, R. S., Sarma, B., Jurovitzki, A. L., and Misra, M. (2015). Fabrication and characterization of titania nanotube/cobalt sulfide supercapacitor electrode in various electrolytes. *Chem. Eng. J.* 260, 671–683. doi:10.1016/j.cej.2014.07.031

Salunkhe, R. R., Ahn, H., Kim, J. H., and Yamauchi, Y. (2015). Rational design of coaxial structured carbon nanotube–manganese oxide (CNT–MnO_2) for energy storage application. *Nanotechnology* 26, 204004. doi:10.1088/0957-4484/26/20/204004

Sarma, B., Ray, R. S., Mohanty, S. K., and Misra, M. (2014). Synergistic enhancement in the capacitance of nickel and cobalt based mixed oxide supercapacitor prepared by electrodeposition. *Appl. Surf. Sci.* 300, 29–36. doi:10.1016/j.apsusc.2014.01.186

Sawangphruk, M., and Limtrakul, J. (2012). Effects of pore diameters on the pseudocapacitive property of three-dimensionally ordered macroporous manganese oxide electrodes. *Mater. Lett.* 68, 230–233. doi:10.1016/j.matlet.2011.10.096

Shinde, S. K., Dubal, D. P., Ghodake, G. S., Gomez-Romero, P., Kim, S., and Fulari, V. J. (2015). Hierarchical 3D-flower-like CuO nanostructure on copper foil for supercapacitors. *RSC Adv.* 5, 30478–30484. doi:10.1039/C4RA11164H

Sui, Z. Y., Wang, C., Shu, K., Yang, Q. S., Ge, Y., Wallace, G. G., et al. (2015). Manganese dioxide-anchored three-dimensional nitrogen-doped graphene hybrid aerogels as excellent anode materials for lithium ion batteries. *J. Mater. Chem. A* 3, 10403–10412. doi:10.1039/C5TA05759K

Sun, K., Wang, H., Peng, H., Wu, Y., Ma, G., and Lei, Z. (2015). Manganese oxide nanorods supported on orange peel-based carbon nanosheets for high performance supercapacitors. *Int. J. Electrochem. Sci.* 10, 2000–2013.

Vijayakumar, S., Ponnalagi, A. K., Nagamuthu, S., and Muralidharan, G. (2013). Microwave assisted synthesis of Co_3O_4 nanoparticles for high-performance supercapacitors. *Electrochim. Acta* 106, 500–505. doi:10.1016/j.electacta.2013.05.121

Wang, C. C., Chen, H. C., and Lu, S. Y. (2014). Manganese oxide/graphene aerogel composites as an outstanding supercapacitor electrode material. *Chem. A Eur. J.* 20, 517–523. doi:10.1002/chem.201303483

Wang, G., Lu, X., Ling, Y., Zhai, T., Wang, H., Tong, Y., et al. (2012). LiCl/PVA gel electrolyte stabilizes vanadium oxide nanowire electrodes for pseudocapacitors. *ACS Nano* 6, 10296–10302. doi:10.1021/nn304178b

Wang, H. Q., Li, Z. S., Huang, Y. G., Li, Q. Y., and Wang, X. Y. (2010). A novel hybrid supercapacitor based on spherical activated carbon and spherical MnO_2 in a non-aqueous electrolyte. *J. Mater. Chem.* 20, 3883–3889. doi:10.1039/c000339e

Wei, H., He, C., Liu, J., Gu, H., Wang, Y., Yan, X., et al. (2015a). Electropolymerized polypyrrole nanocomposites with cobalt oxide coated on carbon paper for electrochemical energy storage. *Polymer* 67, 192–199. doi:10.1016/j.polymer.2015.04.064

Wei, B., Wang, L., Miao, Q., Yuan, Y., Dong, P., Vajtai, R., et al. (2015b). Fabrication of manganese oxide/three-dimensional reduced graphene oxide composites as the supercapacitors by a reverse microemulsion method. *Carbon N. Y.* 85, 249–260. doi:10.1016/j.carbon.2014.12.063

Xia, X. H., Tu, J. P., Zhang, Y. Q., Mai, Y. J., Wang, X. L., Gu, C. D., et al. (2011). Three-dimentional porous nano-Ni/$Co(OH)_2$ nanoflake composite film: a pseudocapacitive material with superior performance. *J. Phys. Chem. C* 115, 22662–22668. doi:10.1021/jp208113j

Xu, J., Gao, L., Cao, J., Wang, W., and Chen, Z. (2010). Preparation and electrochemical capacitance of cobalt oxide (Co_3O_4) nanotubes as supercapacitor material. *Electrochim. Acta* 56, 732–736. doi:10.1016/j.electacta.2010.09.092

Yang, W., Gao, Z., Ma, J., Wang, J., Wang, B., and Liu, L. (2013). Effects of solvent on the morphology of nanostructured Co_3O_4 and its application for high-performance supercapacitors. *Electrochim. Acta* 112, 378–385. doi:10.1016/j.electacta.2013.08.056

Yao, W. L., Wang, J. L., Yang, J., and Du, G. D. (2008). Novel carbon nanofiber-cobalt oxide composites for lithium storage with large capacity and high reversibility. *J. Power Sources* 176, 369–372. doi:10.1016/j.jpowsour.2007.10.073

Yu, G., Xie, X., Pan, L., Bao, Z., and Cui, Y. (2013). Hybrid nanostructured materials for high-performance electrochemical capacitors. *Nano Energy* 2, 213–234. doi:10.1016/j.nanoen.2012.10.006

Yu, Z. J., Dai, Y., and Chen, W. (2009). Synthesis of Co_2O_4 microspheres by hydrothermal-precipitation for electrochemical supercapacitors. *Adv. Mater. Res.* 66, 280–283. doi:10.4028/www.scientific.net/AMR.66.280

Zeng, Z., Zhou, H., Long, X., Guo, E., and Wang, X. (2015). Electrodeposition of hierarchical manganese oxide on metal nanoparticles decorated nanoporous gold with enhanced supercapacitor performance. *J. Alloys Comp.* 632, 376–385. doi:10.1016/j.jallcom.2015.01.240

Zhang, F., Zhang, T., Yang, X., Zhang, L., Leng, K., Huang, Y., et al. (2013). A high-performance supercapacitor-battery hybrid energy storage device based on graphene-enhanced electrode materials with ultrahigh energy density. *Energy Environ. Sci.* 6, 1623–1632. doi:10.1039/c3ee40509e

Zhang, J., and Zhao, X. S. (2012). Conducting polymers directly coated on reduced graphene oxide sheets as high-performance supercapacitor electrodes. *J. Phys. Chem. C* 116, 5420–5426. doi:10.1021/jp211474e

Zhang, X., Sun, X., Zhang, H., Li, C., and Ma, Y. (2014). Comparative performance of birnessite-type MnO_2 nanoplates and octahedral molecular sieve (OMS-5) nanobelts of manganese dioxide as electrode materials for supercapacitor application. *Electrochim. Acta* 132, 315–322. doi:10.1016/j.electacta.2014.03.176

Zhu, S. J., Zhang, J., Ma, J. J., Zhang, Y. X., and Yao, K. X. (2015). Rational design of coaxial mesoporous birnessite manganese dioxide/amorphous-carbon nanotubes arrays for advanced asymmetric supercapacitors. *J. Power Sources* 278, 555–561. doi:10.1016/j.jpowsour.2014.12.054

Conflict of Interest Statement: The authors declare that the research was conducted in the absence of any commercial or financial relationships that could be construed as a potential conflict of interest.

FABRICATION OF SPHERICAL NANOCRYSTALLINE $MnCo_2O_4$ VIA SOL- GEL CITRATE ROUTE FOR SUPERCAPACITOR APPLICATION

Santosh J Uke[1,2], Vijay P. Akhare[2], Satish P. Meshram[3], Devidas R. Bambole[1], Dindayal S. Thakre[1], Gajanan N. Chaudhari[2].

[1*]Department of Physics, J.D.P.S. College, Daryapur, Dist Amravati, Maharashtra, India,

[2]Nanoscience Research Laboratory, Shri. Shivaji Science College, Amravati, Maharashtra, India

[3]Nanomaterials Laboratory, Centre for Materials for Electronics Technology (C-MET), Pune, India

Abstract

Herein present paper, the sol-gel citrate route for synthesis of crystalline $MnCo_2O_4$ nanosphers is reported. The as- synthesized nanocrystalline $MnCo_2O_4$ were characterized by means of X-ray diffraction (XRD), Field emission scanning electron microscopy (FE-SEM), Fourier transform infrared spectroscopy (FTIR) and Brunauer–Emmett–Teller (BET). The XRD analysis reveals the nanocrystalline nature of as-prepared $MnCo_2O_4$ nanocrystals. Electrochemical properties of nanocrystalline $MnCo_2O_4$ have been studied by cyclic voltammetry, Galvanostatic charge–discharge and electrochemical impedance spectroscopy, which showed the maximum specific capacitance of 42.5 F g^{-1}at current density 0.1 $mAcm^{-2}$. The synthesis method used in this study is promising for producing the nanocrystalline material for high performance supercapacitor electrode.

Keywords: Nanocrystalline, capacitor, capacitance.

I. INTRODUCTION

To meet the recent and future challenges in the modern society, the flexible, wearable, lightweight and low cost energy storage system has a very intense demand [i]. In this regards, the world has an ample expectation from the scientific community for finding new energy storage system that fulfils these requirements. Recently, supercapacitor or electrochemical capacitor (EC) is the emerging energy storage systems are currently having intense demands. Supercapacitor is going to overcome the recent commercial energy storage like conventional capacitor and lead acid battery. Supercapacitor has many attractive features such as high power density, high energy density, lightweight, fast charging-discharging rate, a good shelf life, secure operation and long life span etc. [ii,iii]. The supercapacitor is used in various applications such as hybrid vehicles, military services and power backup, portable electronics like laptops, mobile phones, wrist watches, wearable devises, roll-up displays electronic papers, etc.[iv,v].

An electrode plays a very important role in the supercapacitor. Depending upon the electrode material used, the supercapacitors are divided into two categories: electrochemical double layer supercapacitor (EDLCs) and pseudocapacitor [vi]. In (EDLCs), the electrode material have been used as SWNT [vii], MWNT [viii], reduced graphine oxide [ix], porous carbon [x], etc., and the specific capacitance arises from the non-Faradaic charge storage mechanism between electrode and electrolyte interface. In pseudocapacitor, the electrode materials that have been used as electrode are transition metal oxides, and the specific capacitance arises from Faradaic reaction at the electrode interface [xi].

The transition metal oxides such as RuO_2, Fe_3O_4, Co_3O_4, MnO_2, Mn_3O_4, CeO_2, Fe_2O_3 etc., and the ternary metal such as $MnCo_2O_4$, $NiCo_2O_4$, $ZnFe_2O_4$, $ZnCo_2O_4$, $CoFe_2O_4$,

$CuFe_2O_4$ and $NiFe_2O_4$ etc., has been widely studied and employed as promising electrode material for pseudocapacitors [xii].

Among these ternary metal oxides, the $MnCo_2O_4$ is the most explored potential candidate in view point of electrode material for supercapacitor owing to its excellent electrochemical properties, natural abundance, cost effectiveness and environmentally compatible nature. In this context several researchers have reported the remarkable results. Sun *et. al.* [xiii] have reported the hydrothermally synthesized $MnCo_2O_4$/C electrode material for water splitting and all state solid supercapacitor application with high specific capacitance of 846 $mFcm^{-2}$ at current density 20μ A cm^{-2}.

Further, Yaun *et al.* [xiv] have reported the one step hydrothermal rout synthesis of $MnCo_2O_4$/reduced graphene oxide nanocomposites for supercapacitor with specific capacitance $334Fg^{-1}$ at current density $1Ag^{-1}$. Sahoo *et al.* [xv] have reported the one-step electrodeposition approach for the synthesis of $MnCo_2O_4$ and reported the specific capacitance of 290 Fg^{-1} at scan rate $1mVs^{-1}$.

In the present report, we have synthesized the $MnCo_2O_4$ via sol-gel citrate method. The synthesized material was characterized using XRD, FE-SEM, FTIR, UV-visible spectroscopy, BET-BJH etc. The electrochemical investigations for supercapacitor application of fabricated $MnCo_2O_4$ electrode was carried out using cyclic voltammetry, galvonostatic charge discharge and impedance spectroscopy.

II. EXPERIMENTAL

A. MATERIALS AND METHOD

All reagents including $KMnO_4$, $Co(NO_3)$ $6H_2O$ and citric acid ($C_6H_8O_7$) were used as starting material and purchased from Qualigen Sd. fine chemicals Ltd. India. The chemical reagents were of analytical grade and used as received.

B. Synthesis of crystalline $MnCo_2O_4$ nanosphere

Synthesis of nanocrystalline $MnCo_2O_4$was carried out by sol-gel citrate method. Initially, the stoichiometric amount of $KMnO_4$ and $Co(NO_3)$ $6H_2O$ with the molar ratio 1:2 were dissolved in methanol. This solution was stirred for 1 hr using a magnetic stirrer followed by vigorous stirring at 80°C on the hot plate for 3 hrs, which results in highly viscous homogenous thick gel. This gel was further transferred to a pressure bomb. The pressure bomb was sealed and heated up to 120°C for 12h and subsequently cooled to room temperature. The obtained dried samples were further ground and calcined at 550°C up to 6 h using alumina crucible in furnace.

C. FABRICATION OF ELECTRODE

The nanocrystalline $MnCo_2O_4$ material was loaded on stainless steel substrate following the standard protocol used for supercapacitor measurement [xvi,xvii]. For this, the 75 weight % of active material, 15 weight % acetylene black as a conductive additive and 10 weight % Poly vinylidene fluoride (PVDF) as a binder were mixed and ground in mortar to have a homogenous mixture. This mixture was further dispersed in a dimethyl formamide (DMF) to form slurry. This slurry was coated on stainless steel (SS) substrate using doctor blade and dried at 60°C. The electrochemical studies such as cyclic voltammetry, galvonostatic charge discharge and impedance spectroscopy were performed using the CHI 6002C and CHI 604E electrochemical workstation forming an electrochemical cell comprising fabricated electrode as working electrode, platinum as counter electrode and Ag/AgCl as a reference electrode in 1 M Na_2SO_4 electrolyte.

D. CHARACTERIZATION

The structural properties and phase identification of the samples was done by Philips X–ray diffractometer (XRD) with filtered Cu-K_α radiation of wavelength λ= 0.1541874 nm. The morphology was determined by Field emission scanning electron microscopy (FE–SEM) (Model: JSM 6701F, JEOL, Japan). The Fourier transform infrared (FTIR) spectra were recorded using Bruker vertex 70 FTIR spectrometer. The VU- Visible investigation of the material was carried out by using Perkin-Elmer Lamda 750, USA.

III. RESULT AND DISCUSSIONS

A. XRD analysis

To understand the lattice parameter and average crystallite size of the as–synthesized $MnCo_2O_4$ samples, the X-ray diffraction (XRD) analysis was carried out. Fig. 1 shows the typical XRD pattern of as-synthesized $MnCo_2O_4$. From the XRD pattern, the sharp peaks appearing at two theta values 31°, 36.95°, 44.44°, 52.07°, 58.18°, 64.52°, 66.9° and 76.85°

can be assigned to (222), (311), (400), (422), (511), (440), (531) and (533) respectively, and are in well agreement to those of spinel fcc structure with space group Fd3m, (227), [JCPDF 23-1237] [xviii,xix]. Further, no impurity peaks were found in the XRD pattern which indicates the formation of well crystalline $MnCo_2O_4$. The average crystallite size D was calculated using the Deby-Scherrer formula [xx] equation (1), where λ is the characteristic wavelength of Cu-Kα radiation, β is the full width half maxima of the diffraction line at half the maximum intensity and θ is the Braggs diffraction angle. The average crystalline size for the $MnCo_2O_4$ was found to be 32 nm.

$$D = \frac{0.9\lambda}{\beta \times \cos\theta} \qquad (1)$$

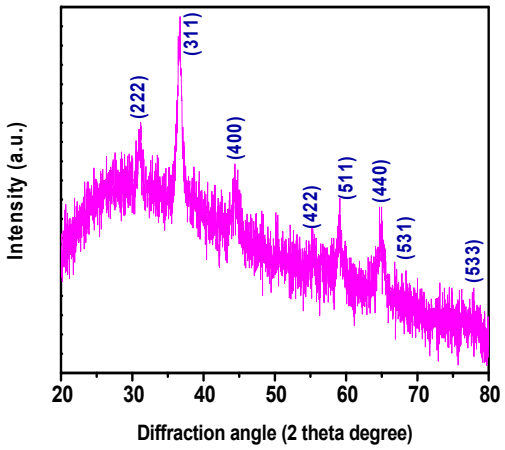

Fig. 1: XRD pattern of nanocrystalline $MnCo_2O_4$

B. FE-SEM analysis

The morphology of as-synthesized nanocrystalline $MnCo_2O_4$ was studied by FE-SEM analysis and the results are shown in Fig. 2. (a) and (b). From high magnification FESEM images (Fig 2(a)-(b)), it can be seen that the as-synthesized product consists of nearly spherical morphology. The nanospheres are formed in large numbers and are separated from each other. The average size of the nanospheres ranges from 29-42 nm which are in close agreement with those of XRD results.

The crystalline nature with spherical morphology of as-synthesized $MnCo_2O_4$ material demonstrated here may exhibit greater surface area and may contribute to electrolyte ion exchange which is one of the prime requirements of high energy storage supercapacitor electrode material.

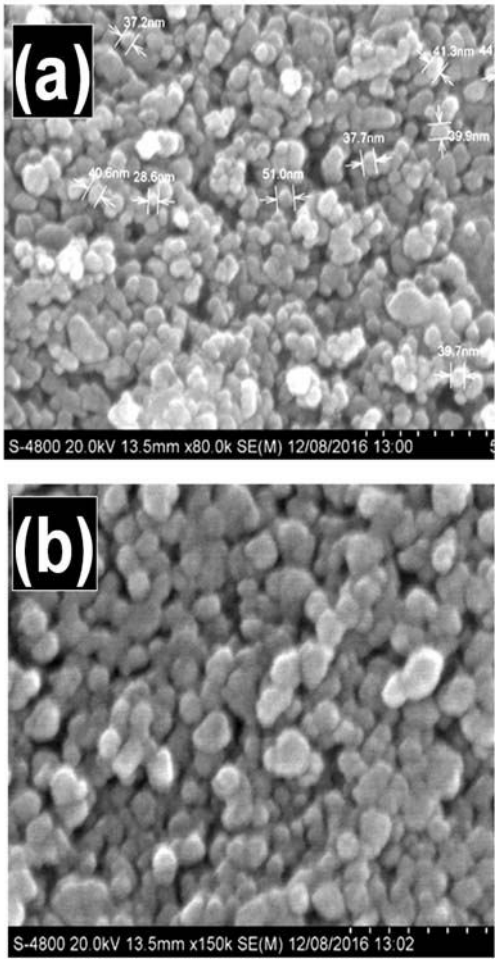

Fig. 2: FE-SEM micrograph of nanocrystalline $MnCo_2O_4$

C. FT-IR analysis

To analyze the bonding and chemical composition of the as synthesized nanocrystalline $MnCo_2O_4$, the Fourier transform infrared spectroscopy (FT-IR) analysis was carried. Fig. 3 shows the FT-IR spectrum of nanocrystalline $MnCo_2O_4$. The broad absorption peak appearing at 2922.59 cm^{-1} and 1609.7 cm^{-1} can be assigned to the O-H of adsorbed water molecule in $MnCo_2O_4$ [xxi,xxii]. The absorption band observed at 1348 cm^{-1} can be ascribed to NO_2 symmetrical stretching in the citrate molecule. The absorption bands at 750–600 cm^{-1} and 600–450 cm^{-1} are due to Mn–O stretching and bending vibrations in the nanocrystalline $MnCo_2O_4$ [xxiii]. The band at 720 cm^{-1} is due to NH_2 wagging from the citrate molecule [xxiv]. The band at680 cm^{-1} can be attributed to the metal oxide bonding [xxv].

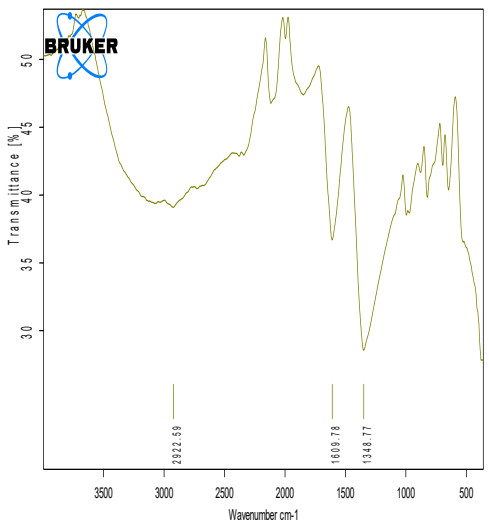

Fig. 3: FTIR spectrum of nanocrystalline $MnCo_2O_4$

D. UV- visible spectroscopy analysis

To investigate the optical band gap in the nanocrystalline $MnCo_2O_4$, the optical study of the as-synthesized nanocrystalline $MnCo_2O_4$ was carried out by using UV–vis spectrophotometer in the wavelength ranges 350–950 nm. The variation in absorption intensity with different wavelengths of nanocrystalline $MnCo_2O_4$ is shown in Fig. 4 (a) and corresponding plot of $(\alpha h\nu)^2$ versus $(h\nu)$ shown in the Fig. 4 (b). The electronic structure and band gap strongly influences the electrochemical properties of the composite material. Fig. 4 (b) shows the strong absorption of nanocrystalline $MnCo_2O_4$ in the 220-250cm^{-1} region. The plot $(\alpha h\nu)^2$ versus $(h\nu)$ (Fig. 4 (b)), which is linear at the absorption edge, further confirms that the material has a direct band gap. The extrapolations of straight line to the energy axis for zero absorption coefficient value give the band gap which was observed to be 4.91 eV. These values are comparable with the theoretical values previously reported in literature [xxvi].

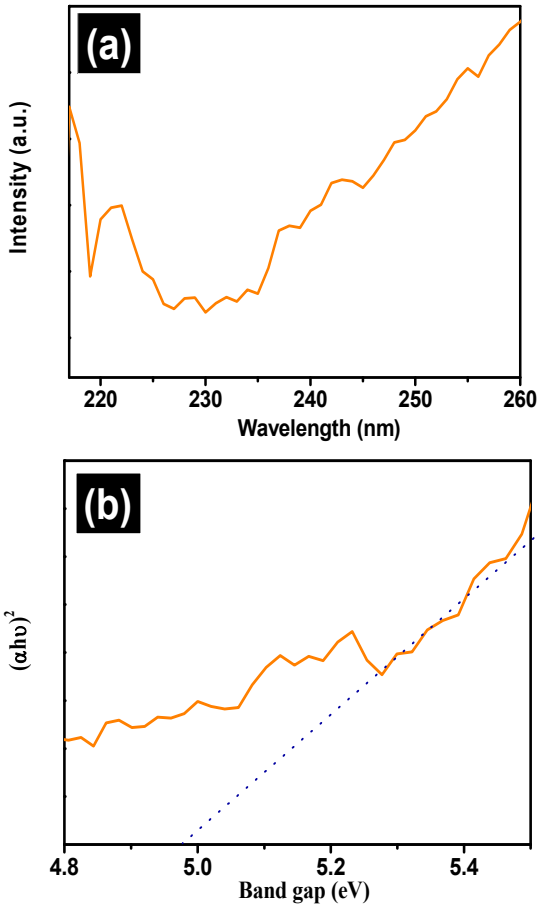

Fig. 4. (a) UV-Visible spectrum and (b) band gap of nanocrystalline $MnCo_2O_4$

E. BET surface area analysis

The Brunauer-Emmett-teller (BET) surface area analysis was carried out to explore the specific surface area of nanocrystalline $MnCo_2O_4$. For this, the N_2 adsorption-desorption isotherm has been carried out. The corresponding results are demonstrated in Fig. 5. From figure, the isotherm with a distinct hysteresis loop in the range of 0 to 1 and at relative pressure *P/Po* canbe clearly seen. The pore size distribution and pore volume of nanocrystalline $MnCo_2O_4$ are estimated using the Barrett-Joyner-Halenda (BJH) method. The pore size distribution of nanocrystalline $MnCo_2O_4$ at the amount of nitrogen absorbed at *P/Po* =0.98595 are shown in inset of Fig. 5. The BET surface area and a corresponding pore volume of the nanocrystalline $MnCo_2O_4$ were found out to be 10.45 m^2g^{-1} and 0.0213 cm^3g^{-1} respectively.

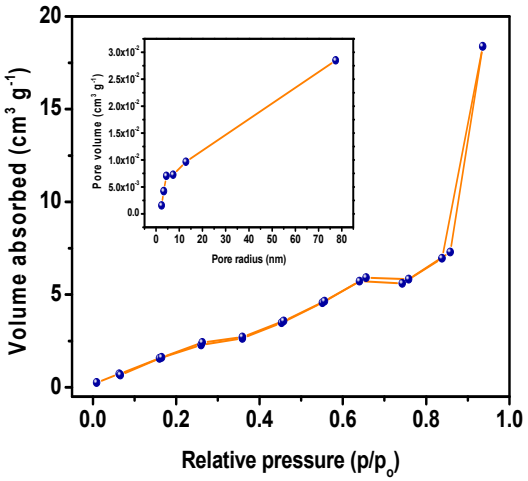

Fig. 5. N_2-adsorption desorption isotherm and the inset shows the corresponding pore size distribution of nanocrystalline $MnCo_2O_4$

F. Electrochemical characterizationanalysis

To understand the electrochemical nature of nanocrystalline $MnCo_2O_4$ electrode, the cyclic voltammetry (CV), galvonostatic charge discharge (GCD) and Electrochemical impedance spectroscopy (EIS) has been carried out in 1 M Na_2SO_4 as electrolyte. The Fig. 6 (a) shows the CV curves of nanocrystalline $MnCo_2O_4$ in the different scan rates of 5 mVs^{-1}, 10 mVs^{-1}, 50 mVs^{-1} and 100 mVs^{-1} in the potential window 0 to 0.6V. The rectangular shape of CV reveals that the specific capacitance is originated from the redox reaction [xxvii]. From CV curves, the values of specific capacitance of nanocrystalline $MnCo_2O_4$ samples at different scan rate are calculated using the equation (2).

$$C_s = \frac{1}{mV(V_c - V_a)} \int_{V_a}^{V_c} I(V)dV \qquad (2)$$

Where m is the mass in (gcm^2) deposited, $I(v)$ is the response current in (mA) of the $MgFe_2O_4$electrode for unit area, V is the scan rate, $(V_c - V_a)$ is the operational potential window in (V), V_a anodic current and V_c cathodic current.

Galvonostatic charge-discharge study of the electrodes of $MnCo_2O_4$ electrode at different current densities 0.1 to 0.5 $mAcm^{-2}$ has been studied using 1M Na_2SO_4 as electrolyte. Fig.6 (b) shows the galvonostatic charge discharge behaviour of the nanocrystalline $MnCo_2O_4$ electrode. The discharge specific capacitance was calculated by galvonostatic charge discharge curves using the equation (3). Additionally, the galvonostatic charge discharge curve is used to measure the energy density and power density of the electrode material, an equation (4) and equation (5) were used to calculate the energy density E (W h Kg^{-1}) and power density P (W Kg^{-1}) respectively,

$$C_s = \frac{T_d \times I_d}{m \times \Delta V} \qquad (3)$$

$$E = \frac{0.5 \times C_s \times (V_{max}^2 - V_{min}^2)}{3.6} \qquad (4)$$

$$P = \frac{E \times 3600}{T_d} \qquad (5)$$

Where Cs (Fg^{-1}) is the specific capacitance, I_d (A) is the current used for Galvonostatic discharge, T_d (s) discharging time, ΔV(V) potential window used for galvonostatic charge discharge and m(g) is the active mass of the electrode [xxviii]. From GCD, the maximum specific capacitance, energy density and power density of $MnCo_2O_4$ electrode at current density 0.1$mAcm^{-2}$ has obtained as 42.5 Fg^{-1}, 2.125W h Kg^{-1} and 137.1kW Kg^{-1}, respectively. Adekunle *et. al.* [xxix] have reported the specific capacitance 11.76 Fg^{-1} for the MWCNT-Co_3O_4/MWCNT asymmetric supercapacitor assembly in 1 M Na_2SO_4. In present reports, the specific capacitance for $MnCo_2O_4$ electrode at current density 0.1mA cm^{-1} was found out to be 42. 5 Fg^{-1}, which is high in comparison with the specific capacitance reported in the literature.

Further, the retention of specific capacitance of the $MnCo_2O_4$ electrode was examined at the current density 0.3 $mAcm^{-2}$ over 1000 cycles. Fig 7 (a) shows the curve for cycle number versus percentage capacity retention for $MnCo_2O_4$ electrode. From figure, it can be seen that the $MnCo_2O_4$ electrode shows the 95.23% retention of specific capacitance over 1000 cycles.

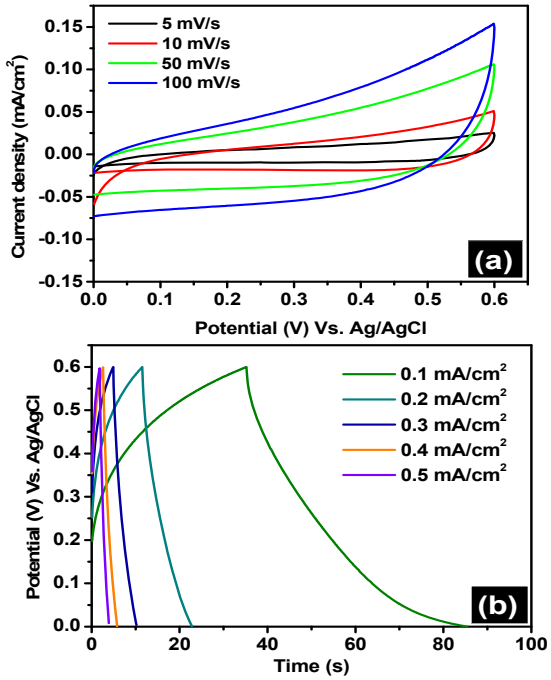

Fig. 6. (a) Cyclic voltammogram (CV), (b) Galvonostatic charge discharge (GCD) of nanocrystalline $MnCo_2O_4$

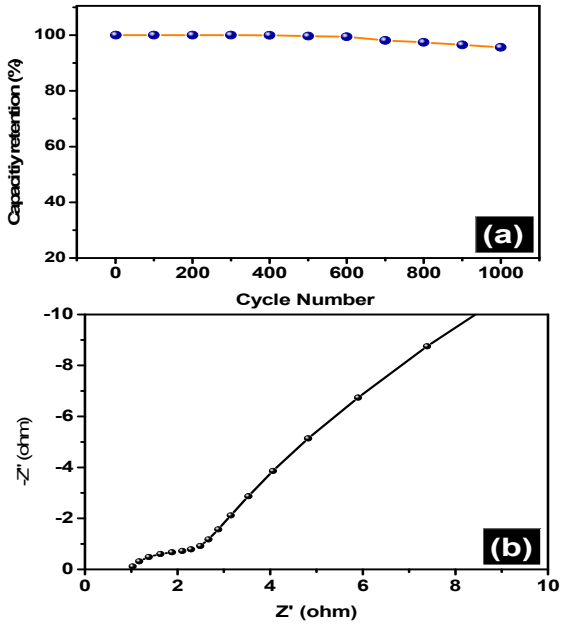

Fig. 7. (a) Capacity retention vs. cycle number at 0.3 $mAcm^{-2}$ and (b) Nyquist plot of nanocrystalline $MnCo_2O_4$

The electrolyte resistance (R_s), the charge–transfer resistance (R_{ct}), the ion transport properties within the interface between the electrode and electrolyte was investigated with the help of electrochemical impedance spectroscopy (EIS). The ESI was investigated within the frequency range 1 Hz to 1 MHz at AC amplitude of 5 mV in 1 M Na_2SO_4 electrolyte.

The typical Nyquist plot for the $MnCo_2O_4$ nanostructure is shown in Fig. 7 (b). The high–frequency intercept of the semi–circle on the real axis yields the electrolyte resistance (R_s) or equivalent series resistance, and the diameter provides the charge–transfer resistance (R_{ct}) over the interface between the electrode and electrolyte [xxx]. The electrolyte resistance (R_s), the charge–transfer resistance (R_{ct}), of the nanostructure $MnCo_2O_4$ was found out to be 2 Ωcm^{-2} and 1.24 Ωcm^{-2}respectively. The low electrolyte resistance(R_s) and the charge–transfer resistance (R_{ct}) of the electrode material are mostly responsible for the result of ion exchange between electrode and electrolyte interface [xxxi]. Fig.8 (a) shows the Bode plot (Phase (Ω cm^{-2}) vs. Frequency (Hz)) of as-synthesized $MnCo_2O_4$ nanostructure.

At low frequency, the phase angle of the electrodes reached to the 45° implies the idea capacitive behavior of the electrode. The characteristic frequency f_o of a phase angle of 45° is ~100 Hz for the $MnCo_2O_4$ nanostructure. The relaxation time constant t_o, is calculated from the equation $t_o=1/f_o$, it was found out to be ~ 0.01. Thus, ESI analysis of nanostructure $MnCo_2O_4$ is in good agreement with the results obtained from CV and GCD.

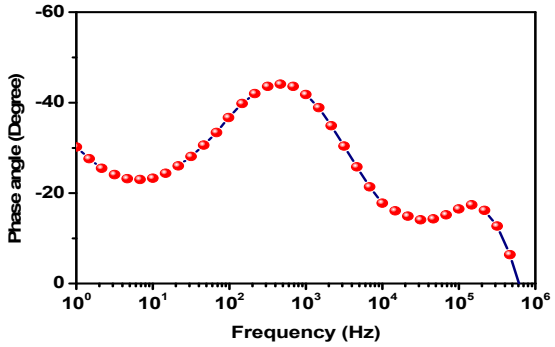

Fig.8 (a) shows the Bode plot (Phase (Ω cm^{-2}) vs. Frequency (Hz)) for nanostructure $MnCo_2O_4$

IV. CONCLUSION

In conclusion, we have successfully synthesized the nanocrystalline $MnCo_2O_4$ via cost effective sol-gel citrate method. The nanocrystalline $MnCo_2O_4$ shows the excellent electrochemical performance in 1M Na_2SO_4 electrolyte. The electrochemical impedance spectroscopy reveals that the nanocrystalline $MnCo_2O_4$ is promising electrode material for high performance supercapacitor. Moreover, the present study demonstrates simple, cost effective sol-gel citrate method for fabrication

of uniform nanocrystalline $MnCo_2O_4$ with very high potential as the electrode for supercapacitor.

V. ACKNOWLEDGMENT

This work is financially supported by University Grant Com-mission (UGC) New Delhi, India under Minor Research Project (File No.47-763/13/WRO) and (File No.47-764/13/WRO).

VI. REFERENSE

[1] Saha, S., Jana, M., Khanra, P., Samanta, P., Koo, H., Murmu, N. C., & Kuila, T. (2016). Band gap modified boron doped NiO/Fe 3 O 4 nanostructure as the positive electrode for high energy asymmetric supercapacitors. RSC Advances, 6(2), 1380-1387.

[2] Uke, S. J., Akhare, V. P., Bambole, D. R., Bodade, A. B., & Chaudhari, G. N. (2017). Recent Advancements in the Cobalt Oxides, Manganese Oxides, and Their Composite As an electrode Material for Supercapacitor: A Review. Frontiers, 4(21), 1

[3] Jayalakshmi, M., & Balasubramanian, K. (2008). Simple capacitors to supercapacitors-an overview. Int. J. Electrochem. Sci, 3(11), 1196-1217..

[4] Wang, G., Lu, X., Ling, Y., Zhai, T., Wang, H., Tong, Y., & Li, Y. (2012). LiCl/PVA gel electrolyte stabilizes vanadium oxide nanowire electrodes for pseudocapacitors. ACS nano, 6(11), 10296-10302.

[5] Lee, S. W., Gallant, B. M., Byon, H. R., Hammond, P. T., & Shao-Horn, Y. (2011). Nanostructured carbon-based electrodes: bridging the gap between thin-film lithium-ion batteries and electrochemical capacitors. Energy & Environmental Science, 4(6), 1972-1985

[6] Uke, S. J., Akhare, V. P., Bambole, D. R., Bodade, A. B., & Chaudhari, G. N. (2017). Recent Advancements in the Cobalt Oxides, Manganese Oxides, and Their Composite As an electrode Material for Supercapacitor: A Review. Frontiers, 4(21), 1.

[7] Liu, T., & Kumar, S. (2006). U.S. Patent No. 7,061,749. Washington, DC: U.S. Patent and Trademark Office.

[8] Huang, K. J., Wang, L., Zhang, J. Z., Wang, L. L., & Mo, Y. P. (2014). One-step preparation of layered molybdenum disulfide/multi-walled carbon nanotube composites for enhanced performance supercapacitor. Energy, 67, 234-240.

[9] Zhang, J., & Zhao, X. S. (2012). Conducting polymers directly coated on reduced graphene oxide sheets as high-performance supercapacitor electrodes. The Journal of Physical Chemistry C, 116(9), 5420-5426.

[10] Kang, D., Liu, Q., Gu, J., Su, Y., Zhang, W., & Zhang, D. (2015). “Egg-Box”-assisted fabrication of porous carbon with small mesopores for high-rate electric double layer capacitors. ACS nano, 9(11), 11225-11233.

[11] Shen, L., Yu, L., Yu, X. Y., Zhang, X., & Lou, X. W. D. (2015). Self-templated formation of uniform NiCo2O4 hollow spheres with complex interior structures for lithium-ion batteries and supercapacitors. Angewandte Chemie International Edition, 54(6), 1868-1872.

[12] Vadiyar, M. M., Bhise, S. C., Kolekar, S. S., Chang, J. Y., Ghule, K. S., & Ghule, A. V. (2016). Low cost flexible 3-D aligned and cross-linked efficient ZnFe 2 O 4 nano-flakes electrode on stainless steel mesh for asymmetric supercapacitors. Journal of Materials Chemistry A, 4(9), 3504-3512.

[13] Sun, C., Yang, J., Dai, Z., Wang, X., Zhang, Y., Li, L., ... & Dong, X. (2016). Nanowires assembled from MnCo2O4@ C nanoparticles for water splitting and all-solid-state supercapacitor. Nano Res, 9, 1300-1309.

[14] Yuan, Y., Bi, H., He, G., Zhu, J., & Chen, H. (2013). A facile hydrothermal synthesis of a MnCo2O4@ reduced graphene oxide nanocomposite for application in supercapacitors. Chemistry Letters, 43(1), 83-85.

[15] Sahoo, S., Naik, K. K., & Rout, C. S. (2015). Electrodeposition of spinel MnCo2O4 nanosheets for supercapacitor applications. Nanotechnology, 26(45), 455401.

[16] Biswal, M., Banerjee, A., Deo, M. and Ogale, S., 2013. From dead leaves to high energy density supercapacitors. Energy & Environmental Science, 6(4), pp.1249-1259.

[17] Yang, X., Sun, H., Zhang, L., Zhao, L., Lian, J. and Jiang, Q., 2016. High Efficient Photo-Fenton Catalyst of α-Fe2O3/MoS2 Hierarchical Nanoheterostructures: Reutilization for Supercapacitors. Scientific reports, 6, p.31591.

[18] Krishnan, S. G., Reddy, M. V., Harilal, M., Vidyadharan, B., Misnon, I. I., Ab Rahim, M. H., ... & Jose, R. (2015). Characterization of

MgCo 2 O 4 as an electrode for high performance supercapacitors. Electrochimica Acta, 161, 312-321.
[19] Liu, H., & Wang, J. (2012). Hydrothermal synthesis and electrochemical performance of MnCo2O4 nanoparticles as anode material in lithium-ion batteries. Journal of electronic materials, 41(11), 3107-3110.
[20] Warren, B.E. and Averbach, B.L., 1952. The separation of cold-work distortion and particle size broadening in X-ray patterns. Journal of Applied Physics, 23(4), pp.497-497.
[21] Raut, S. S., & Sankapal, B. R. (2016). First report on synthesis of ZnFe 2 O 4 thin film using successive ionic layer adsorption and reaction: approach towards solid-state symmetric supercapacitor device. Electrochimica Acta, 198, 203-211.
[22] Infrared spectroscopy : Fundamental and application ;Barbara Stuart, Wiley
[23] Sun, M., Ye, F., Lan, B., Yu, L., Cheng, X., Liu, S., & Zhang, X. (2012). One-step Hydrothermal Synthesis of Sn-doped OMS-2 and Their Electrochemical Performance. Int. J. Electrochem. Sci, 7, 9278-9289.
[24] Shinde, S. S., Gund, G. S., Dubal, D. P., Jambure, S. B., & Lokhande, C. D. (2014). Morphological modulation of polypyrrole thin films through oxidizing agents and their concurrent effect on supercapacitor performance. Electrochimica Acta, 119, 1-10.
[25] Ma, L., Shen, X., Ji, Z., Cai, X., Zhu, G., & Chen, K. (2015). Porous NiCo 2 O 4 nanosheets/reduced graphene oxide composite: Facile synthesis and excellent capacitive performance for supercapacitors. Journal of colloid and interface science, 440, 211-218..
[26] Habibi, M. H., & Fakhri, F. (2017). Hydrothermal synthesis of nickel iron oxide nano-composite and application as magnetically separable photocatalyst for degradation of Solar Blue G dye. Journal of Materials Science: Materials in Electronics, 1-6.

[27] Dubal, D. P., Chodankar, N. R., Holze, R., Kim, D. H., & Gomez-Romero, P. (2017). Ultrathin Mesoporous RuCo2O4 Nanoflakes: An Advanced Electrode for High-Performance Asymmetric Supercapacitors. ChemSusChem, 10(8), 1771-1782.
[28] Xu, K., Yang, J., Li, S., Liu, Q. and Hu, J., 2017. Facile synthesis of hierarchical mesoporous NiCo 2 O 4 nanoflowers with large specific surface area for high-performance supercapacitors. Materials Letters, 187, pp.129-132.
[29] Agboola, B. O., Ebenso, E. E., Oyenkunle, J. A., & Oluwatobi, O. S. (2015). Comparative supercapacitive properties of asymmetry two electrode coin type supercapacitor cells made from MWCNTS/cobalt oxide and MWCNTs/iron oxide nanocomposite.
[30] Dubal, D. P., Lee, S. H., Kim, J. G., Kim, W. B., & Lokhande, C. D. (2012). Porous polypyrrole clusters prepared by electropolymerization for a high performance supercapacitor. Journal of Materials Chemistry, 22(7), 3044-3052.
[31] Xu, K., Yang, J., Li, S., Liu, Q., & Hu, J. (2017). Facile synthesis of hierarchical mesoporous NiCo 2 O 4 nanoflowers with large specific surface area for high-performance supercapacitors. Materials Letters, 187, 129-132

International Journal of Materials Science
ISSN 0973-4589 Volume 12, Number 2 (2017), pp. 371-377

http://www.ripublication.com

Cost effective synthesis of spinel $NiCo_2O_4$ nanocrystal by sol-gel citrate method and its application for supercapacitor

S. J. Uke[ab], V.P. Akhare[b], D.R. Bambole[a], A. B. Bodade[b], G.N. Chaudhary[b]

[a]*J.D.P.S. College, Daryapur, Dist Amravati, Maharashtra-444803, India*

[b]*Nanoscience Research Laboratory, Shri Shivaji .Sscience. College Amravati, Maharashtra-444602, India.*

Abstract

In the present investigation, nanocrystalline spinel $NiCo_2O_4$ was synthesised by simple and cost effective sol-gel citrate method. Synthesized $NiCo_2O_4$ was characterized by using different characterization techniques. The electrochemical supercapacitive performance study shows that $NiCo_2O_4$ exhibits high specific capacitance of 342 Fg^{-1} in 1 M Na_2SO_4 electrolyte with good stability. The further EIS analysis implies low ESR value with excellent frequency response of nanocrystalline $NiCo_2O_4$.Thus present study successfully conveys the applicability of easy and cost effective sol- gel citrate method for synthesis of nanocrystalline $NiCo_2O_4$ to be utilised for supercapacitor.

Keywords: supercapacitor, specific surface area, impedance spectroscopy, specific capacitance

1. INTRODUCTION

Due to the concerns about the depletion of fossil fuel, global warming issues and increasing demand of energy, the development of alternate energy storage resources with high power and energy capacity is of particular interest [1,2]. Among the various energy storage resources, supercapacitor, have attracted immense attention because many attractive properties, such as high energy density, fast charging-discharging and long cycle life [1]. The electrode material is an important part of supercapacitor. At present, the use of nanomaterials as the electrode of supercapacitors has attracted

great interest since they have shown higher power, energy densities and specific surface area than the respective bulk material [3]. The conductivity of the material directly influences the charge stored on the electrodes [4]. The binary transition metal oxides have a much higher electrical conductivity as compared to single transition metal oxides. The binary metal oxides such as $NiCo_2O_4$, $MnCo_2O_4$, $ZnCo_2O_4$, $CuFe_2O_4$, $CoFe_2O_4$, $ZnMn_2O_4$ have been extensively studied for the electrode material in supercapacitor [5].Among the binary metal oxides, $NiCo_2O_4$ is considered as a very promising electrode material for supercapacitor because of its good electrical conductivity, low cost, non toxicity and great flexibility in the structures and morphology [6,7].

This letter is aimed at presenting a more systematic report on the applicability of easy and cost effective sol- gel citrate method for synthesis of nanocrystalline $NiCo_2O_4$ to be utilised for supercapacitor. The specific capacitance of the supercapacitor can be enhanced by increasing the surface area of synthesized material. There are different methods of synthesis of $NiCo_2O_4$ [8,9], out of these different methods of synthesis of nanocrystalline $NiCo_2O_4$, sol- gel citrate method is simple, cost effective and results in high surface area nanocrystals with desire morphology[10].

2. EXPERIMENTAL

Nanocrystalline $NiCo_2O_4$ was synthesised by using sol-gel citrate method. Nickel nitrate and cobalt nitrate were used as starting materials. A stoichiometric mixture of nitrates was mixed with citric acid and ethanol and stirred magnetically at 80^{o}C for 3 h to obtain a homogenous mixture. The solution was further heated at the pressure vessel at about 130^{o}C for 3h. The dried powder was then calcined at temperatures from 350^{o}C to 750^{o}C. Electrode was fabricated by dispersing the nanocrystalline powder of 95 weight % $NiCo_2O_4$ in dimethyl formamide as a solvent and 5 wt % Poly (Vinylidene fluoride) (PVDF) as binder, homogeneous gel formed deposited on stainless still as a substrate via bath deposition method. The electrochemical test of the sample was conducted using a three electrode system in 1 M Na_2So_4 using a CHI 604e electrochemical workstation. The stainless still supported composite was directly used as working electrode with platinum plate counter electrode and Ag/AgCl as a reference electrode.

3. RESULT AND DISCUSSION

Fig 1(a) shows XRD pattern of nanocrystalline $NiCo_2O_4$ synthesised by sol- gel citrate method. It is seen that XRD pattern exhibits major peaks reflecting along the (311), other peaks corresponding to (111), (220), (400), (401), (422), (511) and (440) planes observed with a lower intensity. The XRD pattern of nanocrystalline $NiCo_2O_4$

is in good agreement with that of the standard pattern for $NiCo_2O_4$ (JCPDF File 20-0781) [11].The result indicates that as prepared $NiCo_2O_4$ has spinel structure with polycrystalline in nature. The average crystalline size of $NiCo_2O_4$ is calculated by Deby-Scherrer formula [12] (1) and it is found to be 19 nm.

$$D = \frac{0.9\,\lambda}{\beta\,cos\theta} \tag{1}$$

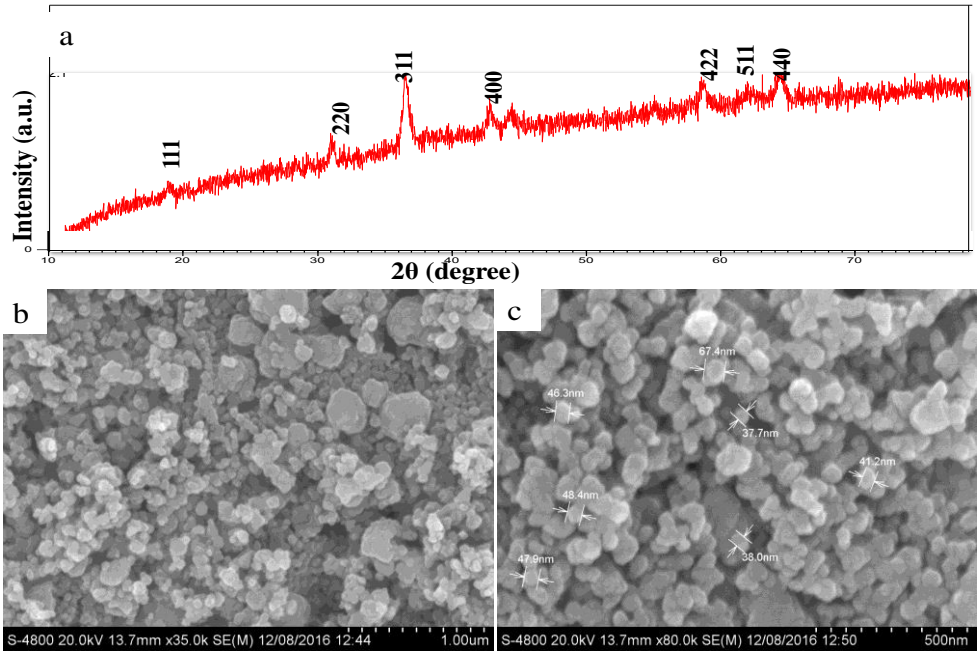

Fig.1. (a) XRD spectra, (b) and (c) FESEM micrograph

The morphology of $NiCo_2O_4$ is investigated by Field emission scanning electron microscopy (FE-SEM). Fig 1 (b) and (c) represent the FE-SEM micrographs of nanocryasalline $NiCo_2O_4$ at two different magnifications. From Fig 1 (b) and (c), it is seen that the random shaped aggregates and agglomeration clusters of $NiCo_2O_4$, the approximate size of which is about 38-68 nm. It is also seen that the size of nanocrystals are uniform, rough and porous with smaller particles suggesting high surface area.

The optical absorption spectrum in the range of 250-280 for $NiCo_2O_4$ is shown in Fig 2 (a). Inset of Fig 2 (a) shows the plot of photon energy (hυ) versus $(\alpha h\upsilon)^2$, which is linear at the absorption edge conforms the material has a direct band gap. The optical band gap value of nanocrystalline $NiCo_2O_4$ estimated from classical relation equation (2) and it is found out to be 4.9 eV.

$$\alpha = \frac{A(h\nu - E_g)}{h\nu} \tag{2}$$

Thermogravimetric and differential thermal analysis (TG-DTA) in the temperature range between room temperature and 700°C were carried out on the nanocrystals of $NiCo_2O_4$ to investigate their thermal behaviour. The corresponding pattern is illustrated in Fig 2 (b). It is seen that, there is no much weight loss is observed with the increase in temperature. This is due to the material was calcined at 550°C and the contained impurities like moisture, structural water, nitrate, CO_2 etc. was already decomposed. The total weight loss is found to be 1.6%. This study confirms that the $NiCo_2O_4$ is thermally stable at higher temperatures and can be applied as the electrode material for supercapacitor at variable temperature applications.

The specific surface area of nanocrystalline $NiCo_2O_4$ has been measured through employing Brunauer-Emmett-teller (BET) method. To study surface area and porosity of nanocrystalline $NiCo_2O_4$ the N_2 adsorption-desorption isotherm has been carried out. The corresponding pattern is illustrated in Fig 2 (c) and (d). Fig 2 (c) shows the isotherm with a distinct hysteresis loop in the range of 0 to 1 and at relative pressure P/P_o. The observed hysteresis loop shifts to higher relative pressure on approaching $P/P_o = 1$, that suggests the hierarchical mesoporous structure of $NiCo_2O_4$. The pore size distribution and pore volume of $NiCo_2O_4$ are estimated using the Barrett-Joyner-Halenda (BJH) method. Fig 2 (d) shows the pore size distribution of $NiCo_2O_4$ at the amount of nitrogen absorbed at P/P_o =0.98595. BET surface area of the $NiCo_2O_4$ is 22.011 m^2/g and a corresponding pore volume is 0.0303 cm^3/g. These results are in good agreement with the literature

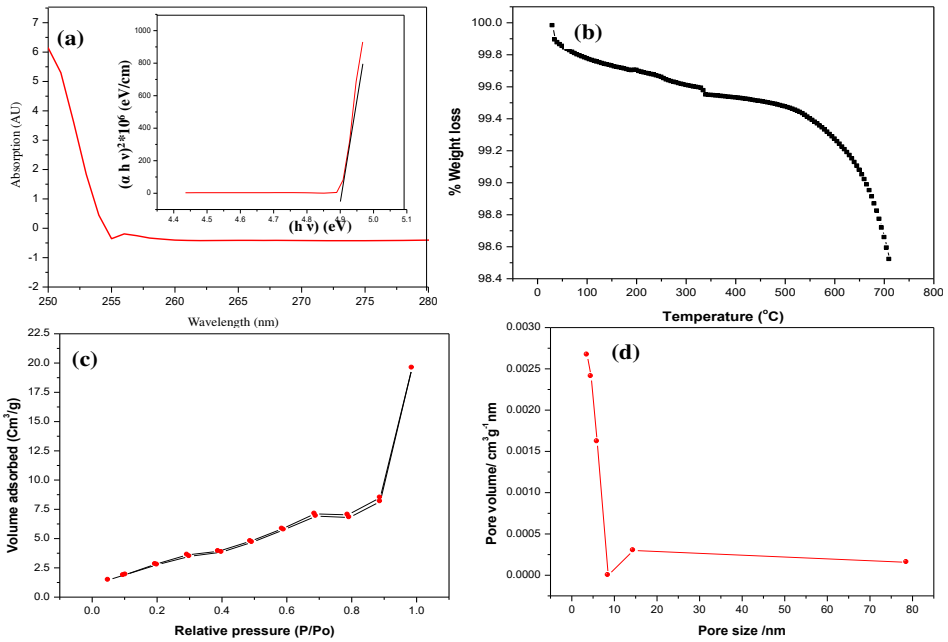

Fig 2 (a) UV- Visible spectra, inset shows the variation of photon energy (hυ) vr $(\alpha h\upsilon)^2$, (b) Thermal analysis (c), N_2 adsorption desorption isotherm and (d) pore size distribution

To estimate the electrochemical behaviour of nanocrystalline $NiCo_2O_4$, Fig 3 (a) gives the cyclic voltrammetric curves for nanocrystalline $NiCo_2O_4$ electrodes in the potential of -0.3 to 0.6V at scan rates 1, 10 and 100 mVs^{-1}in 1M Na_2SO_4 electrolyte. Compared with the curves at different scan rates, all curves shows the pair of oxidation and reduction peaks, which indicates that the current potential response was potential dependant and pseudocapacitance mainly derived from redox reaction of nanocrystalline $NiCo_2O_4$ electrodes. It was found that the current responses as a function of scan rates and the slowly increased with the increase scan rate. This shows that the volatmmetric currents are directly proportional to scan rates of CV. This indicates an ideally capacitive behaviour [13].

The $NiCo_2O_4$ electrode exhibits specific capacitance of 342 Fg^{-1} 248 Fg^{-1} and 13. 3 Fg^{-1} at 1 mVs^{-1} 10 mVs^{-1} and 100 mVs^{-1} scan rates respectively. The maximum specific capacitance and energy density was calculated to be 342 Fg^{-1} and 12.35 W h Kg^{-1} at scan rate $1mVs^{-1}$. Fig 3(b) represents the variation of scan rate with the specific capacitance. As the scan rate increases, the specific capacitance decrease, which is distinctive for electrochemically active $NiCo_2O_4$. As shown in fig 3 (b) the specific capacitance decreases from 342 Fg^{-1} to 13.3 Fg^{-1}. Such behaviour of supercapacitor is due to diffusion effects of protons within the electrodes and presence of inner active sites that cannot sustain the redox transition completely at higher scan rates[14].

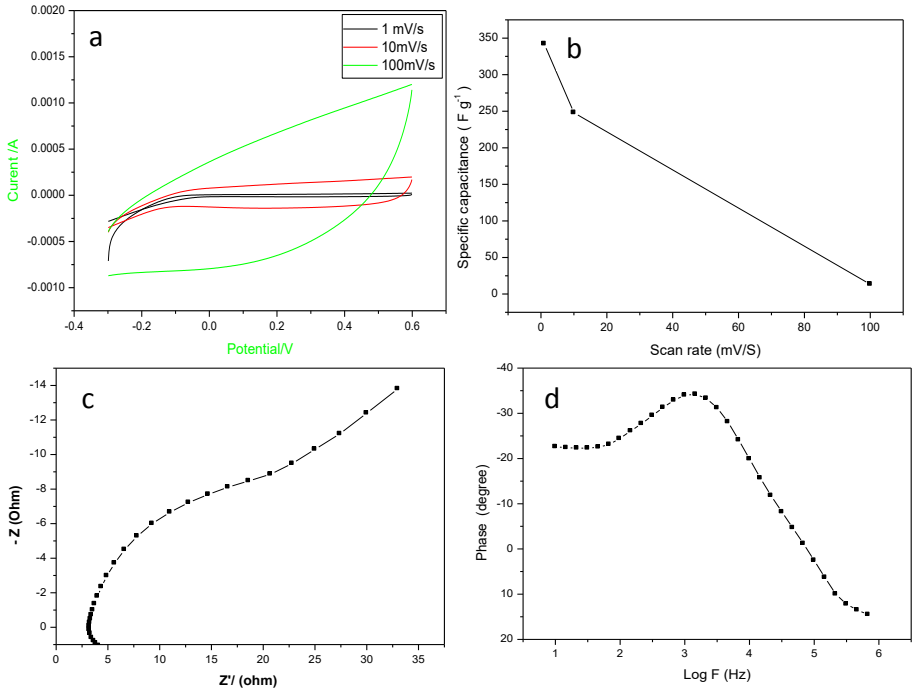

Fig 3 (a) cyclic voltrammogram curve, (b) effect of scan rates on specific capacitance (c) Nyquist plot and (d) Bode plot

Impedance spectroscopic analysis of material was carried out in the frequency range 1Hz to 1MHz. Fig.3 (c) and (d) shows the Nyquist plot (real part vs. imaginary part of impedance) and Bode plots (frequency vs. phase angle) of nanocrystalline $NiCo_2O_4$ respectively. The intercept of the Nyquist plots to the real axis represents equivalent series resistance (R_s) which involves the electrolyte resistance, the intrinsic resistance of the electrode material and the contact resistance of active material to the current collector. The semicircle in the high frequency region gives the charge transfer resistance (R_{ct}), it is related to the internal resistance of the electrode and the double layer capacitance (C_{dl}). The charge transfer resistance (R_{ct}) was calculated by measuring the diameter of the semicircle. [15]. From fig 3 (c) equivalent series resistance (R_s) and charge transfer resistance (R_{ct}) of $NiCo_2O_4$ supercapacitor were found to be 4.7Ω and 15.2Ω respectively. The response-time data are calculated from Bode plot *(frequency Vs Phase).* Fig.3 (d) shows the Bode plot for electrode. These data follow the same trend as internal- resistance values. The ion-diffusion pathway through the layer of porous matrix is responsible for shorter response time [16]. The response time of $NiCo_2O_4$ is found to be less at a constant phase angle.

4. CONCLUSION

In summary, we have successfully synthesised nanocrystalline $NiCo_2O_4$ by cost effective sol-gel citrate method. BET surface area and corresponding pore volume of $NiCo_2O_4$ were found to be 22.011 m^2/g and 0.0303 cm^3/g respectively. The highest specific capacitance and energy density at scan rate 1 mVs^{-1} were achieved to be 342 Fg^{-1} and 12.35 W h Kg^{-1} respectively. ESI study shows the low values of equivalent series resistance and charge transfer resistance are favourable for an increase in the value specific capacitance of $NiCo_2O_4$. Thus the results suggest that the sol-gel citrate method can serve as promising synthesis method for preparation of $NiCo_2O_4$ for high performance supercapacitor.

ACKNOWLEDGMENT

This work was financially supported by University Grant Commission (UGC) New Delhi, India under Minor Research Project (File No.47-763/13/WRO) and (File No.47-764/13/WRO).

REFERENCES

[1] Maa XJ, Konga LB, Zhanga WB, Liua MC, Luob YC, Kang L; Electrochimica Acta 130 ;2014;660–669

[2] Dubal DP, Gund GS, Lokhande CD, Holze R;Materials Research Bulletin;48;2013;923–928

[3] Wang H., Casalongue HS., Liang Y., Dai HJ.;J. Am. Chem. Soc;132;2010;7472.

[4] Snook GA, Kaob P, Best AS. Journal of Power Sources;196;2011;1–12

[5] Suchow L, J. Chem. Educ. 53;1976;560

[6] Yu L, Zhang G, Yuan C, Lou XW, Chem. Commun. 49;2013,137–139

[7] Cui B, Lin H, Li JB, Li X, Yang J, Tao J, Adv. Funct. Mater. 2008;18;1440 – 1447

[8] Pu X, Jin X,Wang J, Cui F, Chu S, Sheng E, Wang Z, J. Electroanal. Chem;707;2014;66.

[9] Hsu HY, Chang KH, Salunkhe RR, Hsu CT, Hu CC, Electrochem. Acta 94;2013;104

[10] Wu YQ, Chen XY, Ji PT, Zhou QQ, Electrochim. Acta;56;2011;7517

[11] Subramani B, Muzhikara PP, Srinivasan A, Rangappa A, Raghavan G, Rao T N, Phys. Chem. Chem. Phys. 2014;16;5284,

[12] Warren, Averbach H ;J. Appl. Phys; 21;1950; 595.

[13] Gujar TP, Shinde VR, Lokhande CD, Kim WY,Jung K.D, Joo O.S., Electrochem. Commun;9;2007;504.

[14] Dubal DP, Dhawale DS, Salunkhe RR, Lokhande CD. J Electroanal Chem;647;2010;60–65.

[15] Chodankar NR, Gund GS, Dubal DP, Lokhande CD, RSC Adv.4;2014;61503–61513

[16] Kumar D, Banerjee A, Patil S, Shukla Ak. Bull. Mater. Sci. 38;6;2015;1507-1517